Design of high-power room-temperature continuous-wave GaSb-based type-I quantum-well lasers with $\lambda > 2.5\ \mu$m

L Shterengas[1]**, G L Belenky**[1]**, J G Kim**[2] **and R U Martinelli**[2]

[1] State University of New York at Stony Brook, Stony Brook, NY 11974-2350, USA
[2] Sarnoff Corporation, CN5300, Princeton, NJ 08543-5300, USA

Abstract

Measurements of gain, loss, threshold current, device efficiency and spontaneous emission of 2.5–2.82 μm In(Al)GaAsSb/GaSb quantum-well diode lasers have been performed over a wide temperature range. The experimental results show that the thermal excitation of holes from the quantum wells into the waveguide where they recombine, but not Auger recombination, limits the continuous-wave room-temperature output power of these lasers, at least up to $\lambda = 2.82\ \mu$m. An approach to extend the wavelength of In(Al)GaAsSb/GaSb diode lasers beyond 3 μm is discussed.

1. Introduction

High power room-temperature (RT) continuous-wave (CW) operation of mid-infrared semiconductor diode lasers is important for many industrial and military applications. Initially, RT diode lasers with $\lambda > 2\ \mu$m were based on double heterostructures with GaInAsSb active regions. The devices emitted in the spectral range of 2.1–2.3 μm with CW output power levels of about 10 mW [1]. Significant performance improvements were achieved through the development of GaInAsSb/AlGaAsSb multiple-quantum-well (MQW) lasers. The devices demonstrated a RT CW power of 190 mW per facet at 2.1 μm [2]. The use of a broadened-waveguide separate-confinement heterostructure (SCH) reduced internal optical loss (α_i) and led to RT AlGaAsSb/InGaAsSb/GaSb type-I MQW lasers with more than 1 W CW at $\lambda \sim 2\ \mu$m [3]. The devices had compressively strained InGaAsSb QWs with In content ∼20%.

The wavelength of RT CW AlGaAsSb/InGaAsSb/GaSb type-I MQW lasers was increased to 2.7 μm by utilizing QWs with up to 40% In content [4]. High-power (160 mW) RT operation was reported up to 2.6 μm. In these lasers the As content of the QW was kept below 2% (quasi-ternary material). This approach is limited to wavelengths below 2.7 μm, owing to strain relaxation in the quasi-ternary QWs that would produce longer wavelengths.

We recently implemented a new design of the AlGaAsSb/InGaAsSb/GaSb type-I MQW lasers. We reported 1 W CW RT operation at 2.5 μm [5]. In these devices, compressive

strain in the In-rich QWs was reduced through the addition of As to the InGaAsSb QWs. Based on the new design, we developed 2.7 μm and 2.8 μm lasers that operated at RT with output powers 500 mW and 160 mW, respectively [6]. The performance degradation with increasing wavelength is usually associated with an increase of Auger recombination.

In this work, we show experimentally that the thermionic excitation of holes from the InGaAsSb QW into, and subsequent recombination within, the AlGaAsSb barrier, and not Auger recombination, are responsible for the degradation of performance with increasing wavelength. We discuss the approaches to increase the wavelength of the GaSb-based high-power RT lasers, including the possibility of using dilute-nitride InGaAs(N)Sb QWs.

2. Laser structures

Laser heterostructures were grown by solid source molecular-beam epitaxy on GaSb substrates. An 800 nm wide $Al_{0.25}Ga_{0.75}As_{0.02}Sb_{0.98}$ broadened-waveguide layer that includes the QWs was sandwiched between two 2 μm wide $Al_{0.9}Ga_{0.1}As_{0.07}Sb_{0.93}$ cladding layers. Details of the lasers' heterostructure design can be found in [5] and [6]. The width and composition of two InGaAsSb QWs, spaced 200 nm apart, determined the wavelength (see table 1). Compressively strained QWs were used to avoid the InGaAsSb miscibility gap, as well as to increase the laser differential gain. All devices were processed into 100 μm aperture, 2 mm long,
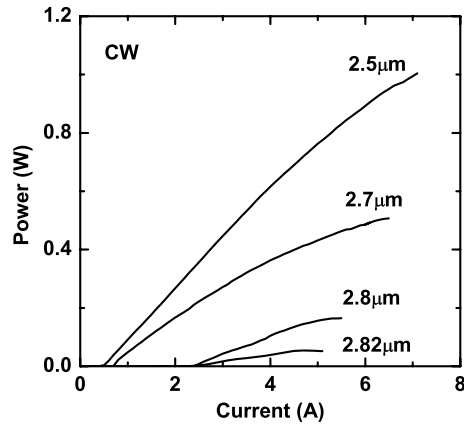
Figure 1. CW light-current characteristics measured at coolant temperatures of 12 and 16 °C for 2.5 and 2.7, 2.8, 2.82 μm lasers, respectively.

Table 1. Width, composition and strain of the QWs for 2.5, 2.7, 2.8 and 2.82 μm lasers.

Wavelength (μm)	QW width (nm)	QW composition	Compressive strain (%)
2.5	14.5	$In_{0.41}Ga_{0.59}As_{0.14}Sb_{0.86}$	1.6
2.7	12	$In_{0.50}Ga_{0.50}As_{0.19}Sb_{0.81}$	1.8
2.8	14.5	$In_{0.50}Ga_{0.50}As_{0.26}Sb_{0.74}$	1.3
2.82	14.5	$In_{0.53}Ga_{0.47}As_{0.30}Sb_{0.70}$	1.2

gain-guided lasers. The facets were coated to reflect 3% and 95%. The devices were In-soldered, epi-side down, onto copper heatsinks.

Figure 1 shows the RT CW light-current characteristics of four lasers with different wavelengths: 2.5, 2.7, 2.8 and 2.82 μm. The maximum CW power decreases with wavelength, from 1 W at 2.5 μm down to 500 mW, 160 mW and 50 mW for the 2.7, 2.8 and 2.82 μm devices, respectively. To achieve the four different wavelengths, the composition and width of the QWs were changed, as shown in table 1. These changes altered carrier confinement in QWs that, in turn, affected the device output power.

3. Results and discussion

To obtain information about recombination mechanisms in the QWs, we measured the spectra of spontaneous emission (SE) from the side of the laser, perpendicular to the output beam. Figure 2(a) shows dependence of SE on laser current (I) for 2.5 μm lasers taken at four temperatures: 200, 240, 280 and 320 K. The slope of SE(I), plotted in double logarithmic scales, is determined by carrier recombination mechanisms. Integrated spontaneous emission is proportional to n^2, where n is the QW electron and hole concentration. Net current through the laser heterostructure is proportional to the sum of all possible recombination currents, i.e., $I \propto An + Bn^2 + Cn^3$, where An is the non-radiative, monomolecular recombination through defects; Bn^2 is the radiative bimolecular recombination; and Cn^3 is the Auger recombination process. The slope of SE(I) decreases with increasing temperature, reaching the value of 0.69 at 320 K.
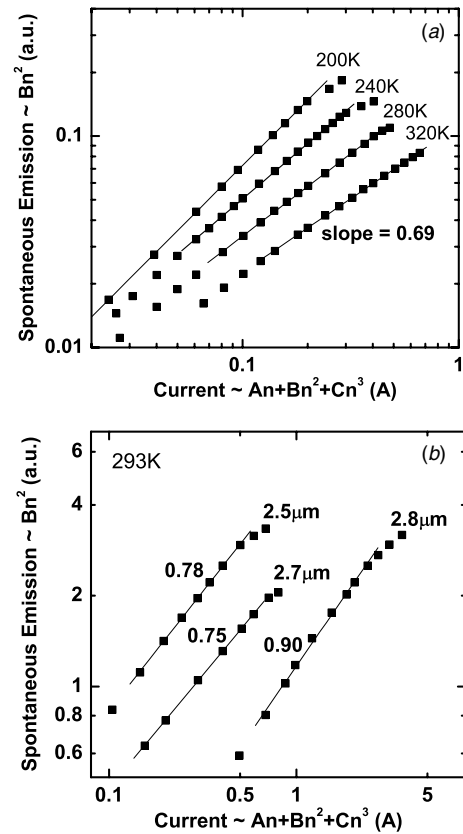

Figure 2. Current dependencies of the spontaneous emission (SE) emitted from the side of the laser for (a) 2.5 μm lasers at 200, 240 280 and 320 K and for (b) 2.5, 2.7 and 2.8 μm lasers at 293 K.

This value corresponds closely to current controlled by Auger recombination, since SE $\sim I^{2/3}$ holds for an Auger-controlled current. It is important to emphasize that 2.5 μm lasers output 1 W CW at RT. Figure 2(b) shows the dependences of SE(I) for 2.5, 2.7 and 2.8 μm lasers measured at 293 K. The slopes of SE(I) are almost identical for 2.5 μm and 2.7 μm devices, at 0.78 and 0.75, respectively. For 2.8 μm devices the corresponding slope is 0.9 that indicates the increasing role of monomolecular recombination. The lattice defects in 2.8 μm material can be anticipated since QW with 50% of In and 26% of As is located close to InGaAsSb miscibility gap. From figure 2 we conclude that Auger recombination cannot account for the decrease of the maximum CW power as the laser wavelength increases from 2.5 to 2.8 μm.

As noted above, the variation of the InGaAsSb QW composition changes the energy barrier for thermionic carrier emission out of the QWs into the $Al_{0.25}Ga_{0.75}As_{0.02}Sb_{0.98}$ waveguide layer. While Auger recombination affects only the threshold current, carrier leakage from the QWs influences both threshold current and external efficiency. We studied the temperature dependence of the laser pulsed (150–200 ns) threshold current and external efficiency (η_{ext}). Characteristic temperatures determined for 2.5, 2.7, 2.8 and 2.82 μm lasers over the temperature range 20–60 °C were T_0: 89, 71, 59, 30 K; T_1: 159, 86, 72, 26 K, respectively. The rapid decrease of T_1 with increasing temperature suggests that carrier leakage contributes to the degradation of the laser thermal performance with increasing wavelength. To investigate the nature of
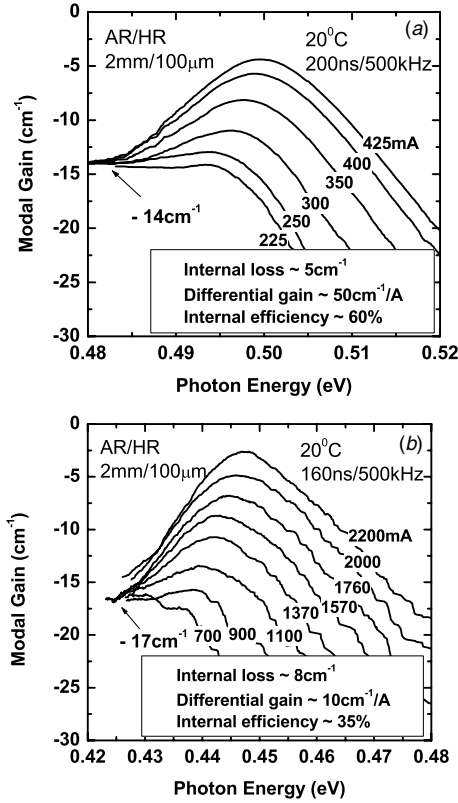
Figure 3. Current dependences of the modal gain spectra for 2.5 μm (*a*) and 2.8 μm (*b*) lasers measured at 20 °C.

Figure 4. Temperature dependence of the internal efficiencies of 2.5, 2.7 and 2.8 μm lasers.

the device temperature performance in more detail, we measured the temperature dependence of the internal efficiency $\eta_i = \eta_{ext}(1 + \alpha_i/\alpha_m)$ for lasers of different wavelengths. The internal efficiency is determined by η_{ext} and the internal losses (α_i) for each device. From the value of the modal gain (figure 3) in the long-wavelength part of the gain spectra, where the material gain is zero, one can determine the total internal loss (α_{tot}). For the mirror loss (α_m) of about 9 cm^{-1} for 2 mm long coated (3%/95%) devices, the internal optical loss for 2.5 and 2.8 μm lasers is 4–5 cm^{-1} and 7–8 cm^{-1}, respectively. Within experimental error, the optical loss is unchanged at temperatures from 200 to 320 K.

The temperature-dependences of η_i for lasers with different wavelengths are presented in figure 4. The results demonstrate that carrier confinement decreases with increasing temperature and with increasing laser wavelength. The decrease of internal efficiency with temperature also contributes to the temperature sensitivity of the laser threshold current and suppresses the laser CW output power (see figure 1). Since the barrier for thermionic emission of electrons from the QWs of our lasers is >400 meV, it is hole leakage from the QWs that reduces the injection efficiency with increasing temperature [7]. We estimated the hole confinement energies following the approach of [8]. The depth of the QWs for holes decreases from about 175 meV for 2.5 μm lasers to 85 meV for 2.8 μm lasers. The increased As content in the QW of long-wavelength lasers causes this barrier energy reduction. Direct measurements of the hole thermal excitation into the n-cladding layer were
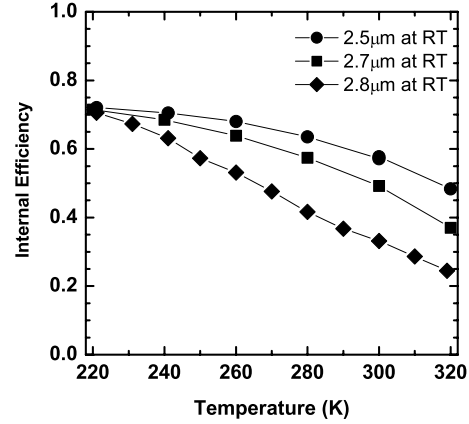
performed using 2.3 μm lasers with similar structures [9], and no significant thermally excited leakage current was recorded. We conclude that the thermionic emission of holes from QWs into, and subsequent recombination within, the barriers is responsible for the decrease of the laser internal efficiency with temperature and with increasing laser wavelength. Since hole leakage from the QWs is greater in lasers with longer wavelength, these devices exhibit a greater deterioration in performance with increasing temperature.

These results demonstrate that the laser performance degradation with increasing wavelength shown in figure 1 is not fundamental and that a design modification can improve the lasers' CW performance. Hole confinement in QWs can be improved by increasing the Al-content of the barrier-layer material. The use of Al$_{0.4}$Ga$_{0.6}$As$_{0.04}$Sb$_{0.96}$ barrier layers should increase hole QW depth by approximately 90 meV, thus providing more temperature-insensitive performance and thereby boosting output power.

The new approach to extend the lasing wavelength beyond 3 μm is to utilize InGaAs(N)Sb QWs. It was recently shown that incorporating nitrogen into various III–V semiconductors decreases the material band gap at the rate of more than 100 meV per at% [10, 11]. Besides increasing the laser wavelength, the introduction of a small fraction (1–2 at%) of nitrogen into InGaAsSb QW reduces the QW compressive strain and suppresses of the intensity of Auger recombination [11].

The position of the valence band edge of a dilute-nitride (N < 2%) InGaAs(N)Sb QW is almost independent of the nitrogen content, and the band gap reduction comes entirely from a large bowing of the conduction band edge. Therefore, the hole confinement barrier is almost unchanged as the QW band gap decreases. In contrast, for N-free InGaAsSb QWs the band gap decrease is accompanied by a valence-band offset reduction that degrades the CW performance of $\lambda > 2.5$ μm type-I GaSb-based lasers, as was shown above. Our preliminary estimation shows that adding just 1% of nitrogen into In$_{0.5}$Ga$_{0.5}$As$_{0.19}$Sb$_{0.81}$ 2.7 μm laser QW should increase the laser wavelength up to 3.5 μm. Laser emission can reach over 4 μm if the nitrogen content is increased up to 2%.

657

4. Summary

We designed and fabricated 2.7–2.82 μm In(Al)GaAsSb/ GaSb type-I high-power room-temperature operated diode lasers. The maximum continuous-wave output powers for 2.7, 2.8 and 2.82 μm devices were 500 mW, 160 mW and 50 mW, respectively. We demonstrated experimentally that the decrease of power with increasing laser wavelength and temperature is caused by the reduction of the hole confinement and the degradation of the material quality, but not by increased Auger recombination. We suggested a novel design of GaSb-based high-power lasers operating over 3 μm that uses dilute-nitride InGaAs(N)Sb QWs.

Acknowledgment

References

[1] Choi H K and Eglash S J 1991 Room temperature operation at 2.2 μm of GaInAsSb/AlGaAsSb diode lasers grown by molecular beam epitaxy *Appl. Phys. Lett.* **59** 1165

[2] Choi H K and Eglash S J 1992 High-power multiple-quantum-well GaInAsSb/AlGaAsSb diode lasers emitting at 2.1 μm with low threshold current density *Appl. Phys. Lett.* **61** 1154

[3] Garbuzov D Z, Martinelli R U, Lee H, York P K, Menna R J, Connolly J C and Narayan S Y 1996 Ultralow-loss broadened waveguide high-power 2 μm AlGaAsSb/InGaAsSb/GaSb separate-confinement quantum-well lasers *Appl. Phys. Lett.* **69** 2007
Turner G W, Choi H K and Manfra M J 1998 Ultralow-threshold (50 A/cm^2) strained single-quantum-well GaInAsSb/AlGaAsSb lasers emitting at 2.05 μm *Appl. Phys. Lett.* **72** 876

[4] Garbuzov D Z, Lee H, Khalfin V, Martinelli R, Connolly J C and Belenky G L 1999 2.3–2.7 μm room temperature CW operation of InGaAsSb/A1GaAsSb broad waveguide SCH-QW diode lasers *IEEE Photonics Technol. Lett.* **11** 794

[5] Kim J G, Shterengas L, Martinelli R U, Belenky G L, Garbuzov D Z and Chan W K 2002 Room-temperature 2.5 μm InGaAsSb/AlGaAsSb diode lasers emitting 1 W continuous-wave *Appl. Phys. Lett.* **81** 3146

[6] Kim J G, Shterengas L, Martinelli R U and Belenky G L 2003 High-power room-temperature continuous wave operation of 2.7 and 2.8 μm In(Al)GaAsSb/GaSb diode lasers *Appl. Phys. Lett.* **83** 1926

[7] Liau Z L and Choi H K 1994 InAs$_{1-x}$Sb$_x$/In$_{1-y}$Ga$_y$As for improved 4–5 μm multiple-quantum-well heterostructure design lasers *Appl. Phys. Lett.* **64** 3219

[8] Krijn M P C M 1991 Heterojunction band offsets and effective masses in III–V quaternary alloys *Semicond. Sci. Technol.* **6** 27

[9] Donetsky D V, Belenky G L, Garbuzov D Z, Lee H, Martinelli R U, Taylor G, Luryi S and Connolly J C 1999 Direct measurements of heterobarrier leakage current and modal gain in 2.3 μm double QW p-substrate InGaAsSb/AlGaAsSb broad area lasers *IEE Electron. Lett.* **35** 298

[10] Kondow M, Kitatani T, Larson M C, Nakahara K, Uomi K and Inoue H 1998 Gas-source MBE of GaInNAs for long-wavelength laser diodes *J. Cryst. Growth* **188** 255
Ha W, Gambin V, Bank S, Wistey M, Yuen H, Kim S and Harris J S 2002 Long-wavelength GaInNAs(Sb) lasers on GaAs *IEEE J. Quantum Electron.* **38** 1260
Harman J-C, Caliman A, Rao E V K, Largeau L, Ramos J, Teissier R, Travers L, Ungaro G, Theys B and Dias I F L 2002 GaNAsSb: how does it compare with other dilute III–V-nitride alloys *Semicond. Sci. Technol.* **17** 778

[11] Murdin B N, Kamal-Saadi M, Lindsay A, O'Reilly E P, Adams A R, Nott G J, Crowder J G, Pigeon C R, Bradley I V, Wells J-P R, Burke T, Johnson A D and Ashley T 2001 Auger recombination in long-wavelength infrared InN$_x$Sb$_{1-x}$ alloys *Appl. Phys. Lett.* **78** 1568